Isolated versus Condensed Anion Structure IV: An NOR Study and X-ray Structure Analysis of $[H_3N(CH_2)_3NH_3]CdI_4 \cdot 2H_2O$, $[H_3CNH_2(CH_2)_3NH_3]CdBr_4$, $[(CH_3)_4N]_2CdBr_4$, and $[(CH_3)_3S]_2CdBr_4$ *

Hideta Ishihara^a, Keizo Horiuchi^b, Shi-qi Dou^c, Thorsten M. Gesing^c, J.-Christian Buhl^c, Helmut Paulus^a, and Hartmut Fuess^d

^a Faculty of Culture and Education, Saga University, Honjo-machi 1, Saga 840-8502, Japan

Z. Naturforsch. 53a, 717-724 (1998); received March 11, 1998

The phase I of $[H_3N(CH_2)_3NH_3]CdI_4 \cdot 2H_2O$ (1) crystallizes with isolated $[CdI_4]^2$ tetrahedra; monoclinic, C2/c, Z=8, a=1702.6(3), b=1459.3(3), c=1555.5(3) pm, and $\beta=120.32(3)^\circ$ at 299 K. (1) shows a first-order phase transition at $T_{1 \leftrightarrow II} = 245$ K. The eight $^{127}I(\nu_1)$ NQR lines in phase II change discontinuously into four lines in phase I. The transition entropy from DSC measurements, $\Delta S=5.0$ J K $^{-1}$ mol $^{-1}$, shows that this transition is probably due to order-disorder of cations. $[H_3CNH_2(CH_2)_3NH_3]CdBr_4$ (2) crystallizes with isolated $[CdBr_4]^2$ tetrahedra; orthorhombic $P2_12_12_1$, Z=4, a=1447.8(5), b=1280.3 (4), c=709.7 (3) pm at 299 K. (2) shows four 81 Br NQR lines between T_1 and around 325 K, above which temperature the lines disappear $I(CH_3)_1NI_2CdBr_4$. (3) shows a sec-Z = 4, a = 144/.8(5), b = 1280.3(4), c = /09.7(3) pm at 299 K. (2) shows four ° Br NQR lines between 77 and around 325 K, above which temperature the lines disappear. [(CH₃)₄N]₂CdBr₄(3) shows a second-order phase transition at $T_{1 \leftrightarrow II} = 271$ K. Three of four ⁸¹Br NQR lines in phase II disappear below this transition point, the other line can be observed up to 315 K. The transition entropy, $\Delta S = 9.01$ J K⁻¹ mol⁻¹, indicates that the transition is an order-disorder type of the cations. [(CH₃)₃S]₂ CdBr₄ (4) shows a first-order type phase transition at $T_{1 \leftrightarrow II} = 304$ K. The four lines spectrum of ⁸¹Br NQR is observed in phase II and disappears above the transition point. The transition entropy, $\Delta S = 46.8$ J K⁻¹ mol⁻¹ is abnormally large. The role of the hydrogen bond and the bridging power between the halogen and cadmium atoms upon the formation of the condensed anion structure is disbetween the halogen and cadmium atoms upon the formation of the condensed anion structure is discussed.

Introduction

We have studied the influence of the cations on the condensation of the anions in the salts (A')MIBr₄ and $(A)_2M^{II}Br_4$ (M = Cd, Zn) by Br NQR and X-ray crystal structure determinations [1-3]. The role of the hydrogen bonds on the formation of the condensed anion structures is pronounced. In order to confirm this conclusion, we prepared complexes with cations without hydrogen atoms involved in hydrogen bonds or which have other groups hindering the formation of hydrogen bonds. In addition, the bridging power of the halogen ligands is also important for the formation of the complex. $[H_3N(CH_2)_3NH_3]CdX_4$ (X = Cl, Br) have layered structures [2, 4]. Therefore, we prepared the iodide analogue in order to compare the briding power. During this study the phase transitions of the title compounds were observed. We report here the NOR results of these four compounds and the crystal structures of [H₃N(CH₂)₃ NH₃|CdI₄ · 2H₂O and [H₃CNH₂(CH₂)₃NH₃|CdBr₄.

Experimental

The title compounds were synthesized from 1,3-propanediamine, N-methyl-1,3-propanediamine, tetramethylammonium bromide, trimethylsulphonium bromide, CdCO₃, and HI or HBr. The components were mixed in stoichiometric ratio in a solution of HI or HBr at pH < 3. The solvents were withdrawn by P_2O_5 in a desiccator. The results of the chemical analyses (in weight %, found/ calculated) are as follows: (1): C, 4.95/4.92; H, 2.07/2.20; N, 3.79/3.82. (2): C, 9.00/9.20; H, 2.66/2.70; N, 5.17/ 5.36. (3): C, 16.17/16.55; H, 4.14/4.16; N, 4.62/4.82. (4): C, 12.26/12.29; H, 3.15/3.09; N, 0.02/0.00. Small single crystals for the X-ray diffraction experiments were grown from aqueous solutions. The structures were determined using a four circle X-ray diffractometer (Stoe-Stadi 4).

Reprint requests to Prof. H. Ishihara; E-mail: ishihara@cc.saga-u.ac.jp

b College of Science, University of the Ryukyus, 1 Senbaru, Nishihara, Okinawa 903-0213, Japan Institut für Mineralogie, Universität Hannover, Welfengarten 1, D-30167 Hannover

d Fachbereich Material wissenschaft, Fachgebiet Strukturforschung, Technische Universität Darmstadt, Petersenstraße 23, D-64287 Darmstadt

^{*} Presented at the XIth NQI International Symposium.

Table 1. Experimental conditions for the crystal structure determinations and crystallographic data of 1,3-propanediammonium tetraiodocadmate (II) dihydrate, $[H_3N(CH_2)_3NH_3]CdI_4 \cdot 2H_2O$ (1) and N-methyl-1.3-propanediammonium tetrabromocadmate (II) $[H_3CNH_2(CH_2)_3NH_3]CdBr_4$ (2). Diffractometer: Stoe-Stadi 4; wavelength: 71.069 pm (MoK α); Monochromator: Graphite (002); scan $2\omega/\theta$. (1): $C_3H_{16}CdI_4N_2O$, M=732.2O, (2): $C_4H_{14}Br_4CdN_2$, M=522.2O

Compound	(1)	(2)
Crystal size/(mm) ³ Temperature/K Absorption coeff./m ⁻¹		6.00 × 0.52 × 0.17 299 (2) 13422
θ-range for data collected	$2.00 \le \theta/^{\circ} \le 28.08$	$2.12 \le \theta/^{\circ} \le 25.00$
Index ranges	$-18 \le h \le 22$ $-17 \le k \le 19$ $-20 \le l \le 20$	$ \begin{array}{l} -17 \le h \le 17 \\ -15 \le k \le 10 \\ 0 \le l \le 8 \end{array} $
Lattice constants a/pm b/pm c/pm c/pm $\alpha/^{\circ}$ $\beta/^{\circ}$ $\gamma/^{\circ}$ $V \cdot 10^{-6}/(pm)^3$ Space group Formula units Z $\rho_{\rm calc}/(Mg \cdot m^{-3})$ $F(000)$ Reflections collected Symmetry independent $[R_{\rm int}]$ Data $(F_0 > 4\sigma(F_0))$ Restraints/Parameters Goodness of fit on F^2	1702.6(3) 1459.3(3) 1555.5(3) 90.00 120.32(3) 90.00 3336.17(9) C ⁶ _{2h} - C2/c 8 2.987(2) 2672.0 22279 3998 0.08 2306	1447.8 (5) 1280.3 (4) 709.7 (3) 90.00 90.00 90.00 1315.5 (8) D ₂ - P2 ₁ 2 ₁ 2 ₁ 4 2.637 (2) 960.0 4689 2325 0.0410 2325 0/103 1.059
Final $R(F_0 > 4\sigma(F_0))$	$wR_2 = 0.0822$	$R_1 = 0.0737$ $wR_2 = 0.1896$
R (all data)	$R_1 = 0.0590,$ $wR_2 = 0.1081$	$R_1 = 0.0770, wR_2 = 0.1896$
Flackparameter	-	0.01(3)
Largest diff: (peak, hole)/ (10 ⁻⁶ e(pm) ³)	1.2(2) and -0.8(2)	3.48 and –3.22
Extincition coeff.	0.0133(7)	0.0038(8)
Point positions:	C ₂ , C ₄ atoms are in 4e, and others in 8f	all atoms are in 4a

From the measured intensities, corrected for Lorentz-polarization and absorption factors, the structures were determined by direct methods, Fourier syntheses, and least squares analysis with the programs given in [5]. The ¹²⁷I and ⁸¹Br NQR spectra were recorded by an NQR spectrometer working in the superregenerative mode. DSC was carried out above 130 K with a differential scanning calorimeter DSC220 from Seiko Instruments Inc. under the following conditions: sample weight ca. 10 mg, the

Table 2. Atomic coordinates and equivalent isotropic displacement parameters $U_{\rm eq}$ (in pm²) for $[{\rm H_3N(CH_2)_3NH_3}]{\rm CdI_4} \cdot 2{\rm H_2O}$ (1) and $[{\rm H_3CNH_2(CH_2)_3NH_3}]{\rm CdBr_4}$ (2). $U_{\rm eq}$ is defined as one third of the trace of the orthogonalized tensor $U_{\rm ij}$. The temperature factor has the form: $T = \exp{\{-2\pi^2(U_{11}h^2a^{*2} + U_{22}k^2b^{*2} + U_{33}l^2c^{*2} + 2U_{12}kha^*b^* + 2U_{13}hla^*c^* + 2U_{23}klb^*c^*\}\}$. Atomic coordinates of hydrogen atoms are given elsewhere [6].

Atom	x	у	z	$U_{ m eq}$
[H ₃ N(C	H ₂) ₃ NH ₃]CdI ₄	· 2H ₂ O (1)		
Çd	0.20368(4)	0.76421(4)	0.18180(5)	436(2)
$I_{(2)}^{(1)}$	0.20316(4)	0.57239(4)	0.17276(5)	482(2)
$I_{(2)}^{(2)}$	0.34090(4)	0.82221(4)	0.14840(5)	495(2)
$I^{(3)}$	0.03327(4)	0.83121(4)	0.04123(5)	592(2)
$I^{(4)}$	0.23652(5)	0.80041(4)	0.37071(5)	551(2)
$O_{(2)}^{(1)}$	0.0246(4)	0.3939(4)	0.0826(5)	583(16)
$O_{(1)}^{(2)}$	0.2557(5)	0.5569(4)	0.4302(5)	612(17)
$N^{(1)}$	0.1396(5)	0.9302(5)	-0.0831(5)	538(19)
N ⁽²⁾	0.4227(5)	0.9423(5)	0.5671(6)	653(23)
$C^{(1)}_{(2)}$	0.4315(6)	0.5177(6)	0.1654(8)	616(25)
$C^{(2)}$	0.5000	0.5741(8)	0.2500	511(31)
$C^{(3)}$	-0.0332(6)	0.6138(5)	0.1577(7)	484(22)
C ⁽⁴⁾	0.0000	0.5605(7)	0.2500	410(26)
[H ₃ CNI	H ₂ (CH ₂) ₃ NH ₃]0	CdBr ₄ (2)		
Cd	0.57354(6)	0.30352(8)	0.87714(14)	406(3)
Br ⁽¹⁾	0.5844(1)	0.1033(1)	0.9152(3)	589(5)
$Br^{(2)}$	0.4124(1)	0.3544(1)	1.0065(2)	455(4)
$Br^{(3)}$	0.5936(1)	0.3526(1)	0.5276(2)	464(4)
$Br^{(4)}$	0.7111(1)	0.3896(1)	1.0521(2)	443 (4)
$N^{(1)}$	0.9017(9)	0.4102(11)	0.7916(18)	507(29)
$C^{(1)}$	0.9455(9)	0.3685(13)	0.6161(24)	517(36)
$C^{(2)}$	0.8749(10)	0.3327(12)	0.4699(25)	493 (33)
$C^{(3)}$	0.8316(10)	0.2261(11)	0.5195(22)	467 (33)
$N^{(2)}$	0.7683(7)	0.1947(8)	0.3668(17)	292(22)
$C^{(4)}$	0.7202(10)	0.0946(10)	0.4046(22)	455 (31)

heating rate $2-10 \text{ K min}^{-1}$ with flowing dry N_2 gas at 40 ml min^{-1} .

Results and Discussion

 $[H_3N(CH_2)_3NH_3]CdI_4 \cdot 2H_2O(1)$

1,3-propanediammonium tetraiodocadmate (II) dihydrate (1) crystallizes at room temperature monoclinic with C_{2h}^6 -C2/c; the lattice constants etc. are listed in Table 1 [6]. Table 2 lists the positional coordinates, and equivalent isotropic thermal parameters $U_{\rm eq}$. Intramolecular distances and angles of the anions are given in Table 3. In Fig. 1 the formula unit is drawn with the numbering of the atoms and the thermal ellipsoids. Figure 2 shows the projection of the unit cell onto the *ab* plane. The [CdI₄]²⁻ tetrahedron in (1) is isolated with small dif-

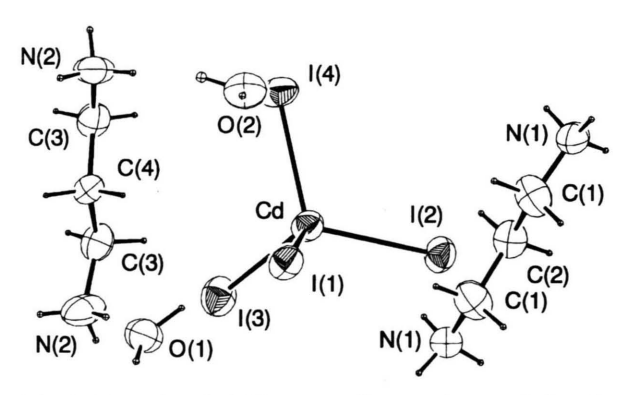


Fig. 1. Formula unit of 1,3-propanediammonium tetraiodocadmate (II) dihydrate (1) with numbering of the atoms. Cations are shown as a whole molecule. The thermal ellipsoids (50% electrons as contour) are shown, too.

ferences in the cadmium-iodine distances, $277.0 \le d$ (Cd-I)/pm \leq 280.3 (mean value 277.7 pm), and the angles in the tetrahedron show small variations, 103.8 ≤ \angle (I-Cd-I)/° \leq 114.0 (mean value 109.4°) as shown in Table 3. The carbon atoms at the center of each 1,3-propanediammonium cation in (1) are located on the 2-fold symmetry. Intramolecular distances and angles in the cations are listed in Table 4. The distances d(N-C) are 145.5 and 146.7 pm, and d(C-C) 147.1 and 149.0 pm. $[CdI_4]^{2-}$ anion layers are on the ac planes situated at b = 0.25and 0.75. Between these layers cations and water molecules are located. Although the N-H and O-H bond distances are fixed at 86 and 95 pm in the refinement, the angles of the N-H···I and O-H···I hydrogen bonds in (1) are listed in Table 3, in consideration of the van der Waals radii of the NH₄ group, the H atom, and the I atom, 160, 120, and 198 pm, respectively [7]. Two N···I hydrogen bonds, $N(1)\cdots I(1')$ and $N(1)\cdots I(3)$, and one $O\cdots I$ hydrogen bond, $O(1)\cdots I(3')$, are formed as shown in Figure 2. Two H₂O molecules are also involved in a series of intermolecular hydrogen bonds (see Table 3). Especially the H₂O⁽²⁾ molecule is located between two ammonium groups, N⁽¹⁾H₃⁺ and N⁽²⁾H₃⁺ groups, and then $H_2O^{(2)}$ is involved in unique hydrogen bonds.

$[N_3CNH_2(CH_2)_3NH_3]CdBr_4(2)$

N-methyl-1,3-propanediammonium tetrabromocadmate (2) crystallizes at room temperature orthorhombic D_2^4 - $P2_12_12_1$; the lattice constants etc. are listed in Table 1. Figure 3 shows the formula unit with numbering of atoms and thermal ellipsoids. Figure 4 shows the projections along [001] on to the *ab* plane. The [CdBr₄]²⁻

Table 3. Intramolecular bond distances (in pm) and bond angles (in degree) for the tetrahedral coordinated CdI_4^{2-} and $CdBr_4^{2-}$ anions, and hydrogen bond scheme.

$[H_3N(CH_2)_3NH_3]CdI_4 \cdot 2H_2O(1)$				
Connection	d/pm	Connection	Angle/°	
Cd-I ⁽¹⁾ Cd-I ⁽²⁾ Cd-I ⁽³⁾ Cd-I ⁽⁴⁾	280.3(1) 277.0(1) 278.4(1) 275.1(1)	I ⁽¹⁾ -Cd-I ⁽²⁾ I ⁽¹⁾ -Cd-I ⁽³⁾ I ⁽¹⁾ -Cd-I ⁽⁴⁾ I ⁽²⁾ -Cd-I ⁽³⁾ I ⁽²⁾ -Cd-I ⁽⁴⁾ I ⁽³⁾ -Cd-I ⁽⁴⁾	106.11(3) 109.62(3) 103.84(3) 112.87(3) 113.95(4) 109.92(4)	

Hydrogen bond scheme

D-H···A	d(H···A)/ pm	d(D···A)/ pm	Angle (D-H···A)/°
$\begin{matrix} O^{(1)}\text{-}H^{(01,1)} \cdots I^{(3')} \\ N^{(1)}\text{-}H^{(N1,2)} \cdots I^{(1')} \\ N^{(1)}\text{-}H^{(N1,3)} \cdots I^{(3)} \\ N^{(1)}\text{-}H^{(N1,1)} \cdots O^{(2')} \\ N^{(2)}\text{-}H^{(N2,2)} \cdots O^{(2'')} \\ N^{(2)}\text{-}H^{(N2,2)} \cdots O^{(1'')} \\ N^{(2)}\text{-}H^{(N2,1)} \cdots O^{(1''')} \end{matrix}$	274.1	368.2	170.2
	298.4	358.9	126.9
	267.0	355.5	173.0
	198.1	282.3	157.3
	226.0	305.9	149.3
	226.6	297.1	136.0
	200.1	289.0	171.6

 $I^{(3')}$: -x, 1-y, -z; $I^{(1')}$: 1/2-x, 3/2-y, -z; $O^{(2')}$: 1/2-x, 1/2+y, 1/2-z; $O^{(2'')}$: 1/2-x, 1/2+y, 1/2-z; $O^{(1''')}$: 1/2-x, 1/2+y, 1/2-z; $O^{(1''')}$: 1/2+x, 3/2-y, 1/2+z.

$[H_3CNH_2(CH_2)_3NH_3]CdBr_4$ (2)

Connection	d/pm	Connection	Angle/°
Cd-Br ⁽¹⁾ Cd-Br ⁽²⁾ Cd-Br ⁽³⁾ Cd-Br ⁽⁴⁾	258.3(2) 259.0(2) 257.6(2) 259.3(2)	Br ⁽¹⁾ -Cd-Br ⁽²⁾ Br ⁽¹⁾ -Cd-Br ⁽³⁾ Br ⁽¹⁾ -Cd-Br ⁽⁴⁾ Br ⁽²⁾ -Cd-Br ⁽³⁾ Br ⁽²⁾ -Cd-Br ⁽⁴⁾ Br ⁽³⁾ -Cd-Br ⁽⁴⁾	105.52(6) 109.63(6) 108.96(7) 112.44(4) 114.53(6) 105.72(6)

Hydrogen bond scheme

D-H···A	d(H···A)/ pm	d(D···A)/ pm	Angle (D-H···A)/°
$\begin{array}{l} N^{(1)} \! \! \! \! \! \! \! \! \! \! \! \! \! \! \! \! \! \! \!$	272.3	333.2	126.7
	263.9	348.2	158.2
	255.1	337.1	153.4
	247.7	343.0	167.7
	261.5	343.2	142.1

 $Br^{(1')}$: x+1/2, -y+1/2, -z+2; $Br^{(2')}$: x+1/2, -y+1/2, -z+1; $Br^{(4')}$: -x+3/2, -y+1, z-1/2.

tetrahedron in (2) is isolated with small differences in the cadmium-bromine distances, $257.6 \le d(\text{Cd-Br})/\text{pm} \le 259.3$ (mean value 258.6 pm), and the angles in the tetrahedron show small variations, $105.5 \le \angle(\text{Br-Cd-Br})/\text{°} \le 112.4$ (mean value 109.5°) as shown in Table 3. Intramolecular distances and angles in the cations are listed in Table 4. The distances d(N-C) are 148 and 150 pm,

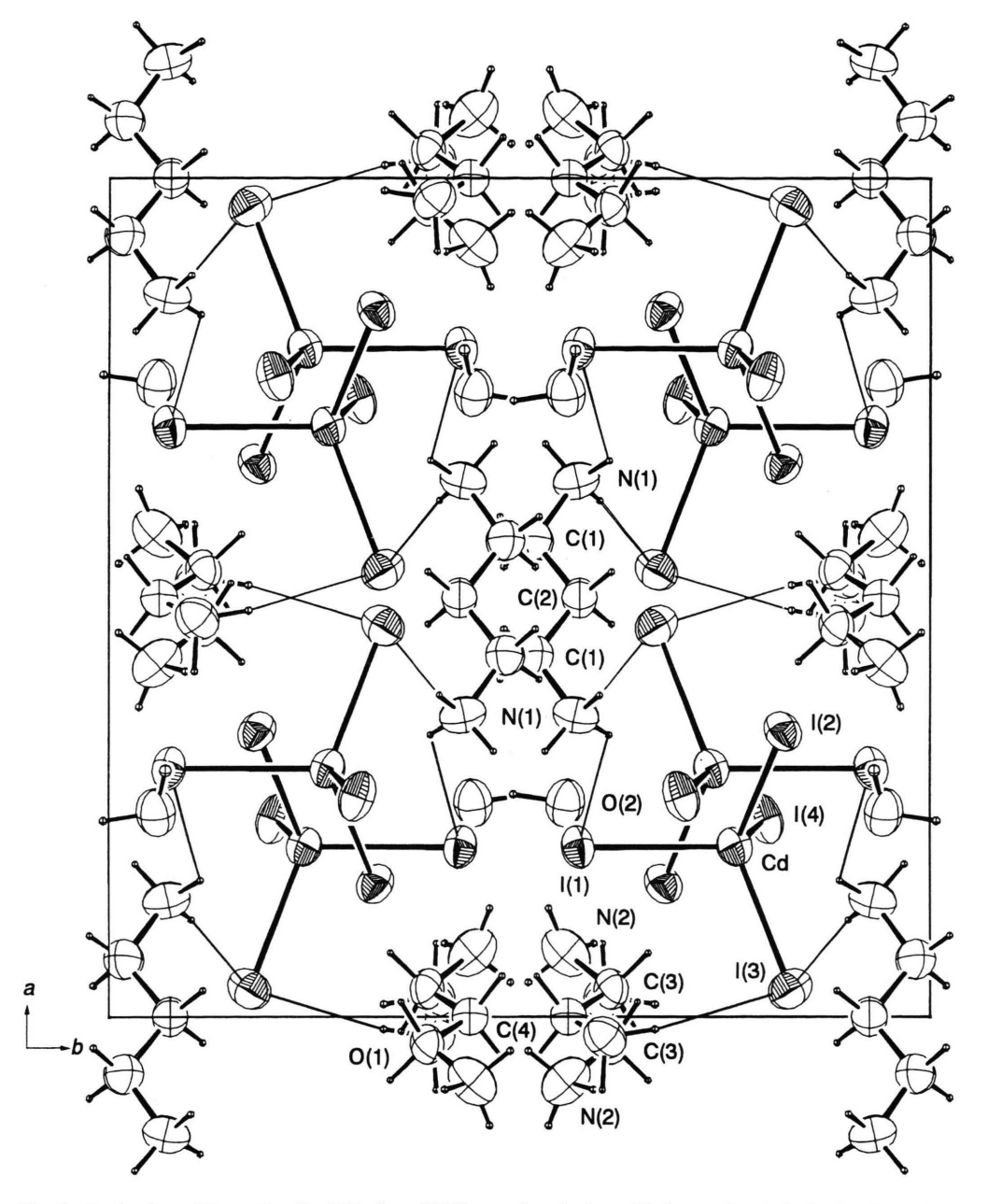
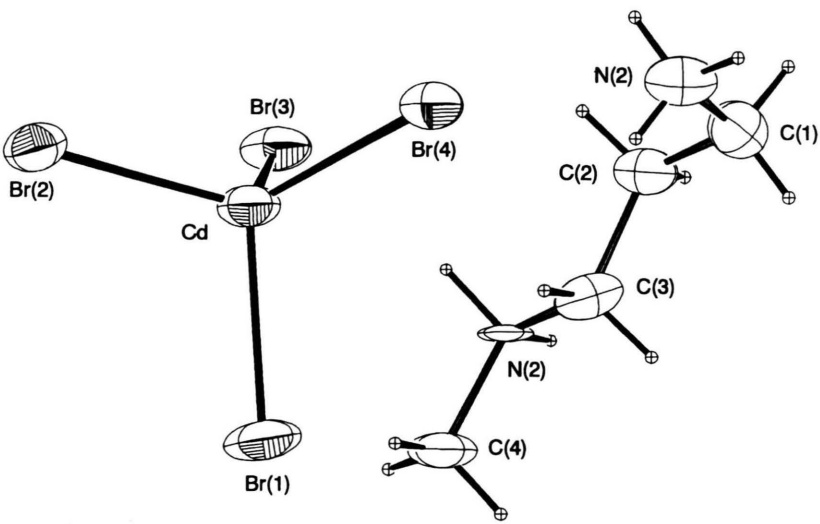


Fig. 2. Projection of the unit cell of (1) along [001] onto the ab plane. Hydrogen bonds including the I atoms are shown by thin lines.

and d(C-C) 153 and 154 pm. The torsion angle of $N^{(1)}$ - $C^{(1)}$ - $C^{(2)}$ - $C^{(3)}$, -76.8° , is strangely small (on the other hand the torsion angles of $C^{(1)}$ - $C^{(2)}$ - $C^{(3)}$ - $N^{(2)}$ is -177.0°). This distortion is due to the molecular packing, because the MO calculation shows the most stable conformation of the $[H_3CNH_2(CH_2)_3NH_3]^{2+}$ ion as all *anti* [8]. In Ta-

ble 3, distances and angles of the N-H···Br hydrogen bonds in (1) are listed in consideration of the van der Waals radii of the NH $_4^+$ group and the Br atom, 160 pm and 190 pm, respectively [7]. The $N^{(2)}H_2$ group forms only two hydrogen bonds of $N^{(2)}\cdots Br^{(2')}$ and $N^{(2)}\cdots Br^{(3)}$ because of the hindrance of the $C^{(4)}H_3$ group. The hydro-



rabromocadmate(II) (2) with the numbering of the atoms. The thermal ellipsoids (50% electrons as contour) are shown, too.

Fig. 3. Formula unit of N-methyl-1,3-propanediammonium tet-

Table 4. Intramolecular distances (in pm) and angles (in degree) within the cations.

$[H_3N(CH_2)_3NH_3]CdI_4 \cdot 2H_2O(1)$			
Connection	d/pm	Connection	Angle/°
N ⁽¹⁾ -C ⁽¹⁾ N ⁽²⁾ -C ⁽³⁾ C ⁽¹⁾ -C ⁽²⁾ C ⁽³⁾ -C ⁽⁴⁾	145.5(11) 146.7(11) 149.0(11) 147.1(11)	N ⁽¹⁾ -C ⁽¹⁾ -C ⁽²⁾ N ⁽²⁾ -C ⁽³⁾ -C ⁽⁴⁾ C ⁽¹⁾ -C ⁽²⁾ -C ^(1') C ⁽³⁾ -C ⁽⁴⁾ -C ^(3')	114.9(7) 113.7(7) 113.0(11) 116.3(11)

C(1'): 1-x, y, 1/2-zC(3'): -x, y, 1/2-z

 $[H_3CNH_2(CH_2)_3NH_3]CdBr_4(2)$

Connection	d/pm	Connection	Angle/°
N ⁽¹⁾ -C ⁽¹⁾ C ⁽¹⁾ -C ⁽²⁾ C ⁽²⁾ -C ⁽³⁾ C ⁽³⁾ -N ⁽²⁾ N ⁽²⁾ -C ⁽⁴⁾	150(2) 153(2) 154(2) 148(2) 148(2)	$N^{(1)}$ - $C^{(1)}$ - $C^{(2)}$ $C^{(1)}$ - $C^{(2)}$ - $C^{(3)}$ $C^{(2)}$ - $C^{(3)}$ - $N^{(2)}$ - $C^{(5)}$	112.9(11) 112.5(14) 109.0(12) 113.2(11)

gen bonds play an important role in the formation of the complex anions [2]. (2) can not form layered complex anions because of the insufficient number of the hydrogen bonds [1-3]. The hydrogen network leads to the layer structure on the ac plane which consists of the [CdBr₄]²⁻ ions and cations as shown in Figure 4. The $N^{(1)} \cdots Br^{(4)}$ hydrogen bonds connect these layers.

Nuclear Quadrupole Resonance and Phase Transition

 $[H_3N(CH_2)_3NH_3]CdI_4 \cdot 2H_2O(1)$ shows eight $^{127}I(v_1)$ NQR lines at 77 K and four lines at 277 K, as listed in

Table 5. 127I and 81Br NQR frequencies at several temperatures for title compounds.

Compounds	T/K	v/MHz	T/K	v/MHz
[H ₃ N(CH ₂) ₃ NH ₃]CdI ₄ · 2H ₂ O (1)	77	v ₁ ^(a) 83.335	277	v ₁ 81.699
. , , , , , , , , , , , , , , , , ,	77	v_1 80.905	277	v_1 78.545
	77	v_1 80.328	277	v_1 76.248
	77	v_1 79.135	277	v_1 67.336
	77	v_1 76.943		
	77	v_1 76.787		
	77	v_1 74.916		
	77	v_1 71.877		
	77	$v_2^{(a)}$ 165.435	294	v_2 162.206
	77	$v_2 = 157.361$	294	v_2 156.429
	77	v_2 156.448	294	v_2 151.013
	77	v_2 153.313	294	v_2 128.604
	77	v_2 150.728		
	77	v_2 150.234		
	77	v_2 141.438		
	77	v_2 138.109		
[H3CNH2(CH2)3NH3]CdBr4 (2)	77	65.784	277	63.516
	77	60.823	277	60.224
	77	60.311	277	59.918
Mark and the second sec	77	59.130	277	57.484
$[(CH_3)_4N]_2CdBr_4$ (3)	77	79.920 ^(b)	279	76.000
	77	79.920 ^(b)		
	77	78.480		
	77	73.921		
$[(CH_3)_3S]_2CdBr_4$ (4)	77	68.502	277	66.246
	77	68.347	277	65.871
	77	64.232	277	61.772
	77	62.511	277	60.850

⁽a) v_1 and v_2 are the NQR line corresponding to the transition $m = \pm 1/2 \leftrightarrow \pm 3/2$ and $m = \pm 3/2 \leftrightarrow \pm 5/2$. (b) a doublet.

Table 5. The temperature dependence of $^{127}I(\nu_1)$ NQR frequencies is shown in Figure 5. The first-order phase transition occurs at 245 K. The eight NOR lines in phase II discontinuously change into four NQR lines in phase I at this transition point. The DSC measurement above 130 K shows the phase transition at 245 K on heat-

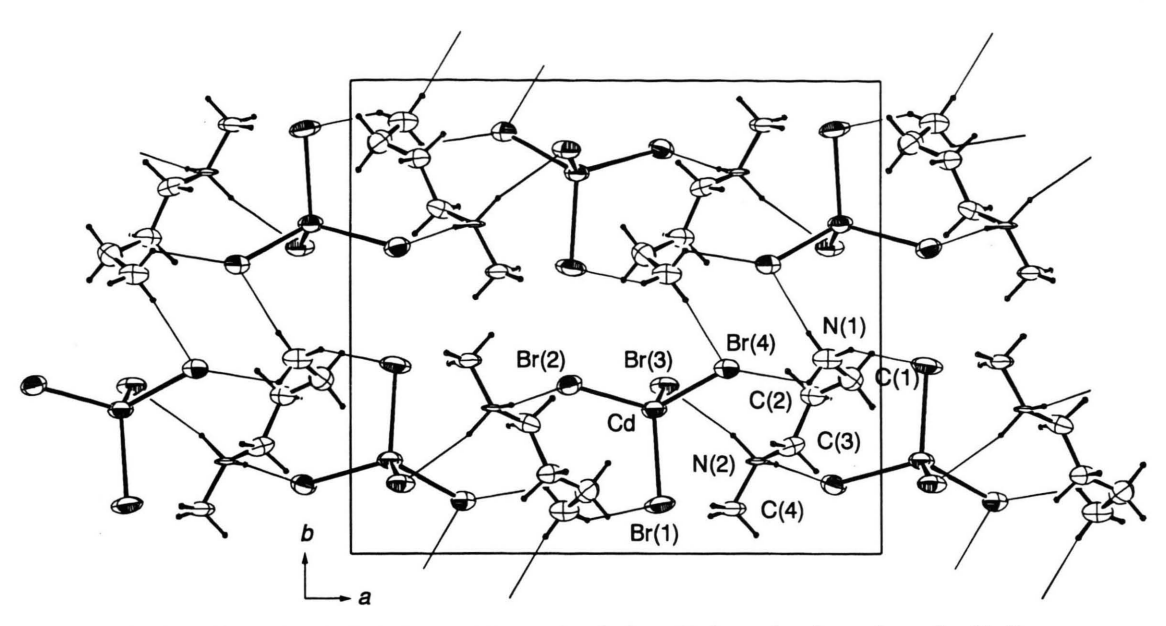


Fig. 4. Projection of the unit cell of (2) along [001] onto the ab plane. Hydrogen bonds are shown by thin lines.

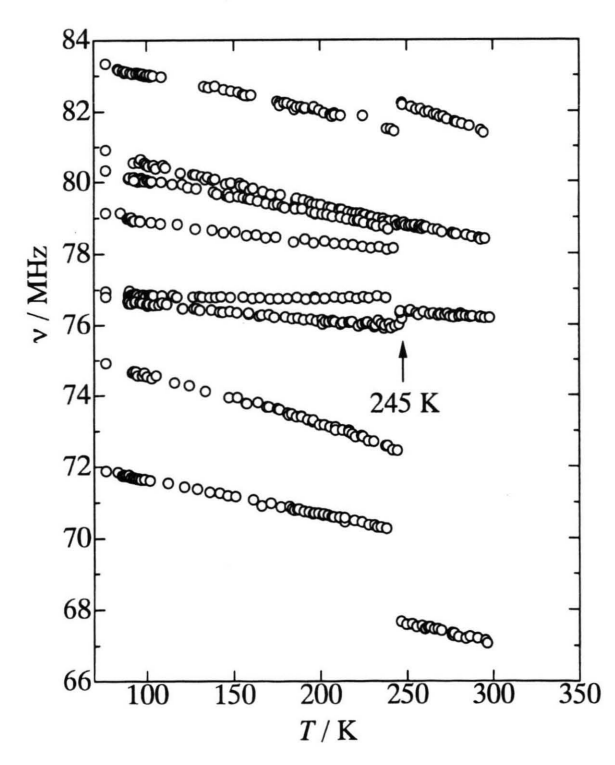


Fig. 5. Temperature dependence of $^{127}I(v_1)$ NQR frequencies of 1,3-propanediammonium tetraiodocadmate(II) dihydrate (1).

ing (the temperature hysteresis was 12 K) and the decomposition over 351 K. The transition entropy ΔS is 5.0 J K⁻¹ mol⁻¹ and thus is nearly $R \ln 2 = 5.8$ J K⁻¹ mol⁻¹. Therefore, this phase transition is probably driven by a split of the cations between the two potential minima.

[H₃CNH₂(CH₂)₃NH₃]CdBr₄ (2) displays four ⁸¹Br NQR lines between 77 and about 325 K, as shown in Figure 6. Four NQR lines disappear above 325 K. The DSC measurement shows no heat anomaly between 130 K and the melting point of 483 K. The disappearance of the NQR lines is probably due to the fluctuation of the electric field gradients at the Br atoms by molecular motion.

[(CH₃)₄N]₂CdBr₄ (3) exhibits four ⁸¹Br NQR lines at 77 K. The temperature dependence of the ⁸¹Br NQR frequencies is shown in Figure 7. A second-order phase transition occurs at 271 K, in good agreement with the result of the DTA [9] and X-ray measurements [10]. Three of the four NQR lines disappear below the transition point. The other line continuously changes at the transition point and is observed up to 315 K. This feature of the temperature dependence of the NQR frequencies is very similar to [(CH₃)₄N]₂HgBr₄ [11] and [(CH₃)₄N]₂ZnBr₄ [12], and these three compounds are isostructural. The transition entropy from the DSC measurement, $\Delta S = 9.0 \text{ J K}^{-1} \text{ mol}^{-1}$, equals almost 2*R*ln2. Therefore we conclude that the transition is of the order-disorder type

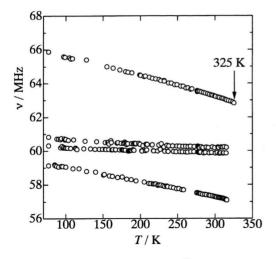


Fig. 6. Temperature dependence of ⁸¹Br NQR frequencies of N-methyl-1,3-propanediammonium tetrabromocadmate (II) (2).

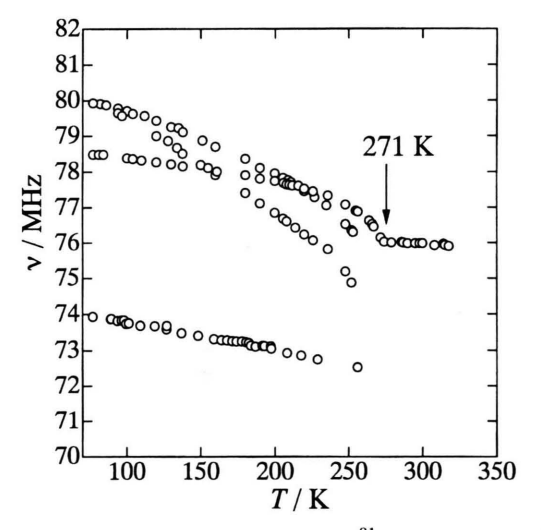


Fig. 7. Temperature dependence of ⁸¹Br NQR frequencies of bis(tetramethylammonium) tetrabromocadmate(II).

with the $[(CH_3)_4N]^+$ cations having two potential minima. On the other hand, Asahi and *et al.* concluded that both anions and cations are disordered above the transition point [10]. The observed crystal structure of the room temperature phase of $[(CH_3)_4N]_2CdBr_4$ [10] shows that the Cd-Br(1) bond is almost parallel to the *c*-axis in space group Pmcn. Under the assumption that the $[CdBr_4]^{2-}$ tetrahedra rotate around the *c*-axis more easily than around the other axes, the electric field gradient (EFG) at the Br(1) site is little affected, while the EFG's at the

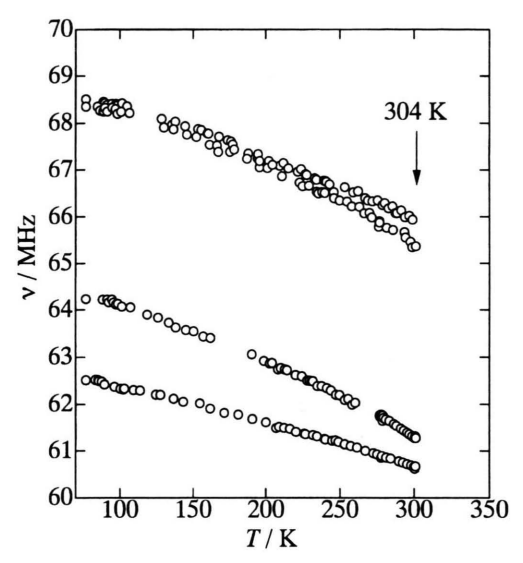


Fig. 8. Temperature of ⁸¹Br NQR frequencies of bis(trimethylsulphonium) tetrabromocadmate(II).

other three bromine sites fluctuate more, making three NQR lines disappear below the transition point. In $[(CH_3)_4N]_2ZnBr_4$ in the room temperature phase (phase I, $T_{1 \leftrightarrow II} = 288$ K [13]), \mathbf{L}_{11} is about two times higher than \mathbf{L}_{22} and \mathbf{L}_{33} (\mathbf{L}_{ii} are the components of the librational tensor \mathbf{L} in the rigid body analysis of the $[ZnBr_4]^{2-}$ tetrahedron) [14] and \mathbf{L}_{11} is also higher than the others even in the low temperature phase [14]. This suggests that the $[ZnBr_4]^{2-}$ tetrahedron executes rotation with large amplitude around the Zn-Br(1) axis, i.e., nearly along the a-axis in the crystal space group Pnma. This explanation probably holds in the case of (3), because (3) shows the same ferroelastic transition with Pmcn \leftrightarrow P2 $_1$ /c sequence (or Pnma \leftrightarrow P2 $_1$ /a sequence) as $[(CH_3)_4N]_2$ $ZnBr_4$ [10, 13].

[(CH₃)₃S]₂CdBr₄ (4) shows four ⁸¹Br NQR lines between 77 and 304 K. All NQR lines disappear above 304 K, as shown in Figure 8. The DSC measurement between 130 K and the melting point of 508 K showed phase transitions at 304 K (the temperature hysteresis was 11 K and $\Delta S = 46.8$ J K⁻¹ mol⁻¹) and 501 K on heating, and (4) decomposes at the melting point. The NQR and DSC results suggest that the phase transition at 304 K is of first-order. The considerably large transition entropy suggests that the phase transition at 304 K is accompanied by a large scale disordering of cations and/or anions in the crystal.

Discussion

 $[H_3N(CH_2)_3NH_3]CdI_4 \cdot 2H_2O$ (1) forms tetrahedral anions, while a perovskite layer structure is detected for $[H_3N(CH_2)_3NH_3]CdBr_4$ [3] and $[H_3N(CH_2)_3NH_3]CdCl_4$ [4]. Although $Cd_2I_6^{2-}$, composed of two edge-sharing CdI_4 tetrahedra, was found [15], it seems that the bridging power of the halogen atoms in the Cd complex is in the order Cl, Br > I. $[(CH_3)_4N]_2CdBr_4$ (3) and $[(CH_3)_3S]_2CdBr_4$ (4) crystallize with cations without hydrogen atoms to form hydrogen bonds of $N\cdots Br$ or $S\cdots Br$ and $[H_3CNH_2(CH_2)_3NH_3]CdBr_4$ (2) with a cation in which the methyl group prevents the formation of hydrogen bonds. All of them show the tetrahedral anion struc-

ture. In addition, the number of hydrogen bonds of $N\cdots I$ in (1) is insufficient, because of the presence of the water molecules. These results suggest that hydrogen bonds play an important role in the formation of the condensed anion structure and that the proper number of hydrogen bonds is necessary for the formation of the perovskite layer structure [1, 2].

Acknowledgements

Two of us, H. I. and K. H., are thankful to the Alexander von Humboldt-Stiftung for a fellowship. The support of the "Fonds der Chemischen Industrie" and of the Deutsche Forschungsgemeinschaft is acknowledged, too.

- H. Ishihara, S. Dou, K. Horiuchi, V. G. Krishnan, H. Paulus, H. Fuess, and Al. Weiss, Z. Naturforsch. 51a, 1027 (1996).
- [2] H. Ishihara, S. Dou, K. Horiuchi, V. G. Krishnan, H. Paulus, H. Fuess, and Al. Weiss, Z. Naturforsch. 51a, 1216 (1996).
- [3] H. Ishihara, S. Dou, K. Horiuchi, H. Paulus, H. Fuess, and Al. Weiss, Z. Naturforsch. 52a, 550 (1997).
- [4] R. D. Willett, Acta Crystallogr. Sect B 33, 1641 (1978).
- [5] G. M. Sheldrick, SHELX86. Program for the solution of crystal structures, University of Göttingen, Germany 1986. SHELX93. Program for crystal structure determination, University of Göttingen, Germany 1993.
- [6] Further information of the crystal structure determinations may be obtained from the Fachinformationszentrum Karlsruhe, Gesellschaft für wissenschaftlich-technische Information mbH, D-76322 Eggenstein-Leopoldhafen, Germany. Inquiries should be accompanied by the depository number CSD-408644 (1) of CSD-408626 (2), the names of the authors and the full literature references.
- [7] A. Bondi, J. Phys. Chem. 68, 441 (1964). L. Pauling, The Nature of the Chemical Bond. 3rd ed., Cornell University Press, Ithaca, New York 1960. Al. Weiss and H. Witte, Kristallstruktur und chemische Bindung. Verlag Chemie, Weinheim 1983.

- [8] MO calculations were performed with the MOPAC93 programm: J. J. P. Stewart, Fujitsu Limited, Tokyo, Japan 1993. Geometry optimization was performed with the PM3 and EF method. The all anti conformer is the most stable one. The conformer in the crystal is less stable by 16.25 kJ mol⁻¹ than the all anti conformer.
- [9] S. Sato, R. Ikeda, and D. Nakamura, Bull. Chem. Soc. Japan 59, 1981 (1986).
- [10] T. Asahi, K. Hasebe, and K. Gesi, J. Phys. Soc. Japan 61, 1590 (1992).
- [11] H. Terao, T. Okuda, K. Yamada, H. Ishihara, and Al. Weiss, Z. Naturforsch. **51a**, 755 (1996).
- [12] R. Perret, Y. Beaucamps, G. Godefroy, P. Muralt, M. Ehrensperger, H. Arend, and D. Altermatt, J. Phys. Soc. Japan 52, 2523 (1983).
- [13] K. Gesi and K. Ozawa, J. Phys. Soc. Japan 52, 2440 (1983).
- [14] P. Trouélan, J. Lefebvre, and R. Derollez, Acta Crystallogr. C40, 386 (1984). P. Trouélan, J. Lefebvre, and R. Derollez, Acta Crystallogr. C41, 846 (1985).
- [15] P. L. Orioli and M. Ciampolini, J. Chem. Soc. Chem. Commun. 1972, 1280.